scientific reports

Check for updates

OPEN

Probenecid inhibits SARS-CoV-2 replication in vivo and in vitro

Jackelyn Murray[1], Robert J. Hogan[1], David E. Martin[2], Kathy Blahunka[2], Fred D. Sancilio[4], Rajiv Balyan[3], Mark Lovern[3], Richard Still[2] & Ralph A. Tripp[1,2]✉

Effective vaccines are slowing the COVID-19 pandemic, but SARS-CoV-2 will likely remain an issue in the future making it important to have therapeutics to treat patients. There are few options for treating patients with COVID-19. We show probenecid potently blocks SARS-CoV-2 replication in mammalian cells and virus replication in a hamster model. Furthermore, we demonstrate that plasma concentrations up to 50-fold higher than the protein binding adjusted IC_{90} value are achievable for 24 h following a single oral dose. These data support the potential clinical utility of probenecid to control SARS-CoV-2 infection in humans.

Severe acute respiratory syndrome coronavirus 2 (SARS-CoV-2) causes coronavirus disease 2019 (COVID-19). In late 2019, the world became aware that SARS-CoV-2 had emerged as a pandemic confirmed by the World Health Organization (WHO) in March 2020. As of late April 2021, there are > 141 million COVID-19 cases with > 3 million deaths worldwide according to the COVID-19 Data Repository by the Center for Systems Science and Engineering (CSSE) at Johns Hopkins University. The SARS-CoV-2 pandemic underscores the urgent need for therapeutics for treatment or prevention as the current armamentarium is comprised of three vaccines[1–3], palliative support, and one antiviral drug, i.e. remdesivir. Remdesivir is a nucleoside analog granted emergency use authorization (EUA) by the FDA based on the demonstration of a decreased time to recovery in patients hospitalized for severe COVID-19[4]. The use of remdesivir is restricted to treating hospitalized, COVID-19 patients via intravenous administration. Vaccines and small molecule therapeutics targeting viruses are the mainstays of antiviral approaches, but complementary approaches targeting host cell genes/processes are needed to reduce the propensity for the development of drug resistance and because targeting host cell pathways can confer broad-spectrum antiviral activity[5,6].

Identifying host cell targets crucial to virus replication is facilitated by high-throughput screening (HTS) methods including the use of RNA interference (RNAi) methodologies[7]. This approach has been used to identify and validate molecular targets and pathways having previously unappreciated antiviral actions, particularly for drug repurposing[6,8]. The repurposing of existing drugs with a known clinical profile has significant advantages over drug discovery as it lowers the risk, time, and cost for development and entry into the clinic[9]. Using HTS to discover host genes required for viral replication, the organic anion transporter 3 (OAT3) gene was identified as a host gene that could be repurposed as a therapeutic candidate[10].

OAT3 is expressed in the kidney, choroid plexus, vascular beds, and other peripheral organs including the lung[11], and mediates the transmembrane transport of endogenous organic anions including urate and other substrates and certain antibiotics[12]. Probenecid {4-[(dipropyl-amino) sulfonyl] benzoic acid} is a commonly used therapeutic agent that inhibits OAT3[13]. Probenecid is a gout treatment, and is a favorable candidate for antiviral drug repurposing, as it is readily commercially available with favorable pharmacokinetics and has a benign clinical safety profile[14]. Probenecid prophylaxis and treatment have been shown to reduce influenza virus replication in vitro in mice[10]. The half-maximal inhibitory concentration (IC_{50}) for treatment of A549 human type II respiratory epithelial (A549) cells infected with A/WSN/33 (H1N1) or A/New Caledonia/20/99 (H1N1) was 5×10^{-4} and 8×10^{-5} μM, respectively[10].

We determined the IC_{50} for Vero E6 cells and normal human bronchoepithelial (NHBE) cells treated before and at the time of infection with SARS-CoV-2 and the B.1.1.7 variant. The results showed probenecid treatment blocked SARS-CoV-2 replication (plaque formation) in Vero E6 cells or NHBE cells treated with different concentrations of probenecid, i.e. 0.00001–100 μM. We also evaluated lung viral load in hamsters on days 0, 3, and 7 pi with SARS-CoV-2 using both a tissue culture infectious dose-50 ($TCID_{50}$) assay and a virus plaque assay to determine the number of plaque-forming units (PFU). Hamsters were treated with probenecid 24 h before infection (prophylaxis), or 48 h post-infection (post-treatment) with doses of 2 mg/kg and 200 mg/kg (Supplementary

[1]Department of Infectious Diseases, University of Georgia, Athens, GA, USA. [2]TrippBio, Inc., Jacksonville, FL, USA. [3]Certara, Princeton, NJ, USA. [4]Department of Chemistry and Biochemistry, Florida Atlantic University, Jupiter, FL, USA. ✉email: ratripp@uga.edu

Fig. 1). Hamsters treated with probenecid had dramatically reduced lung virus titers, i.e. 4–5-log reduction of virus compared to the controls that were approximately 10^9 logs of the virus. We performed a probenecid pharmacokinetic modeling and simulation study comparing 600 mg twice daily, 900 mg twice daily, or 1800 mg once daily. The model predicted that the plasma concentrations of probenecid would exceed the protein binding adjusted IC_{90} value at all time points throughout therapy. The doses evaluated by the PK model were below the maximum allowable FDA-approved dose of 2 g/day and should have no substantial side effects. Together, these data strongly support the potential for probenecid to provide a robust antiviral response against SARS-CoV-2.

Results

After performing RNAi screens in human lung type II epithelial (A549) cells that allowed us to determine and validate host genes required for influenza virus replication[6], we chose to evaluate OAT3[10]. Transfection of A549 cells with siRNA targeting the SLC22A8 gene, OAT3, completely blocked influenza A/WSN/33 (H1N1) virus replication, and probenecid treatment reduced OAT3 mRNA and protein levels in vitro and BALB/c mice. As probenecid treatment in vitro or in vivo did not block influenza virus infection but did block virus titers as measured by plaque assay and hemagglutination assay, we determined the in vitro inhibitory effect on SARS-CoV-2 replication in Vero E6 cells, and NHBE cells (Fig. 1). Vero E6 cells and NHBE cells were pretreated with differing probenecid concentrations and the level of infectious virions in the tissue culture supernatant was determined at 48 h after infection by plaque assay. Probenecid treatment reduced SARS-CoV-2 replication by 90% in NHBE cells (A) or 60% in Vero E6 cells (B). The IC_{50} value for probenecid was shown to be 0.75 μM in Vero E6 cells and 0.0013 μM in NHBE cells. Viability was also assessed over the differing concentrations, demonstrating no cellular toxicity at the highest drug concentration (data not shown). Probenecid treatment was also effective at inhibiting a SARS-CoV-2 variant of concern (VOC), i.e. hCoV-19/USA/CA_CDC_5574/2020, B.1.1.7 (Supplemental Fig. 2). This variant was isolated from a nasopharyngeal swab on December 29, 2020, and after sequencing it to the lineage B.1.1.7 (a.k.a. UK variant). This VOC may have increased transmissibility[16].

Having shown in vitro efficacy and determined the IC_{50} values, we next determined the efficacy of probenecid in the hamster model regarded as a preclinical model of SARS-CoV-2 disease with hamsters having self-limiting pneumonia[17,18]. We examined hamsters infected with SARS-CoV-2 and treated them with probenecid for either 24 h before infection (prophylaxis) or 48 h post-infection (post-treatment). The dosing groups tested were: a) two prophylaxis groups treated with doses of 2 mg/kg or 200 mg/kg, b) two post-treatment groups treated with doses of 2 mg/kg or 200 mg/kg, and two control groups that were SARS-CoV-2 infected or not infected. Disease in hamsters following SARS-CoV-2 infection is transient peaking around day 3–4 post-infection with no clinical signs[17]. Consistent with this observation, no substantial clinical symptoms or weight loss was evident in any group throughout the study (Supplementary Fig. 1). Hamsters treated with probenecid had dramatically reduced lung virus titers (Fig. 2), i.e. a 4–5-log reduction of virus compared to the PBS controls that were approximately 10^9 logs of virus. At day 7 pi all groups cleared the virus in the lungs. RT-qPCR analysis showed low-to-no virus detection at day 7 pi with Ct = 30 except for 2 mg probenecid treatment which was Ct = 28 (Supplementary Fig. 3).

Finally, a population pharmacokinetics (pop-PK) model was developed to characterize probenecid PK. It had a one-compartment structure with saturable elimination and first-order absorption. We performed simulations using the final pop-PK model to generate probenecid exposure profiles comparing 600 mg twice daily, 900 mg twice daily, or 1800 mg once daily administration (Fig. 3 and Table 1). The doses examined are predicted to provide plasma concentrations exceeding the protein binding adjusted IC_{90} value at all time points. All doses were below the maximum allowable FDA-approved dose and are generally safe with no significant side effects.

Discussion

The availability of small-molecule treatments for COVID-19 is limited. Currently, only remdesivir has received EUA approval for treatment of SARS-CoV-219 and it must be administered intravenously in hospitalized patients. There are several additional antivirals in development for the treatment of non-hospitalized patients; however, they have not been able to demonstrate drug exposures significantly greater than the protein binding adjusted IC_{90} value[19–21]. As shown in Table 1, all dose levels of probenecid are projected to exceed the protein binding adjusted IC_{90} value by 14- to 44-fold. Importantly, probenecid has a long and benign safety record over 5 decades of use. Given *the* in vitro efficacy, the in vivo effect in hamsters, the preliminary results from our investigator-initiated study, and the favorable pharmacokinetic results and benign safety profile, probenecid should be considered as a potential treatment option for COVID-19 patients.

Probenecid has inhibitory effects on RNA viruses specifically influenza[10] and respiratory syncytial virus (RSV) (data not shown). Probenecid increases uric acid excretion in the urine and has been safely used to treat gout and hyperuricemia[22,23], and has minimal adverse effects but may cause mild symptoms such as nausea, or loss of appetite[14]. Probenecid has several pharmacological targets including blocking pannexins that underlie transmembrane channel function[24,25] and decreasing ACE2 expression[26,27]. The major advantages of probenecid are that it is an FDA-approved therapeutic drug that has been on the market for > 50 years, it can be administered orally with favorable pharmacokinetics, it operates at the host cell level, is refractory to viral mutation, and has the potential to treat multiple other viruses. Further, our data suggest that initiation of post-treatment following infection in mammalian cells, hamsters, and humans results in infection remarkably reduced SARS-CoV-2 replication, particularly in the lung target organ.

Probenecid treatment will likely have the benefit of inhibiting SARS-CoV-2 variants as we show that it is effective against the VOC, lineage B.1.1.7. This is not unexpected, as targeting host processes essential for viral replication such as OAT3 would be expected to be universal. Among the host targets that have been identified as potential targets for inhibiting virus replication, OAT3 blockade will not likely confer any mechanism-based untoward effects for humans since humans with reduced OAT3 function are healthy[28], and pharmacologic

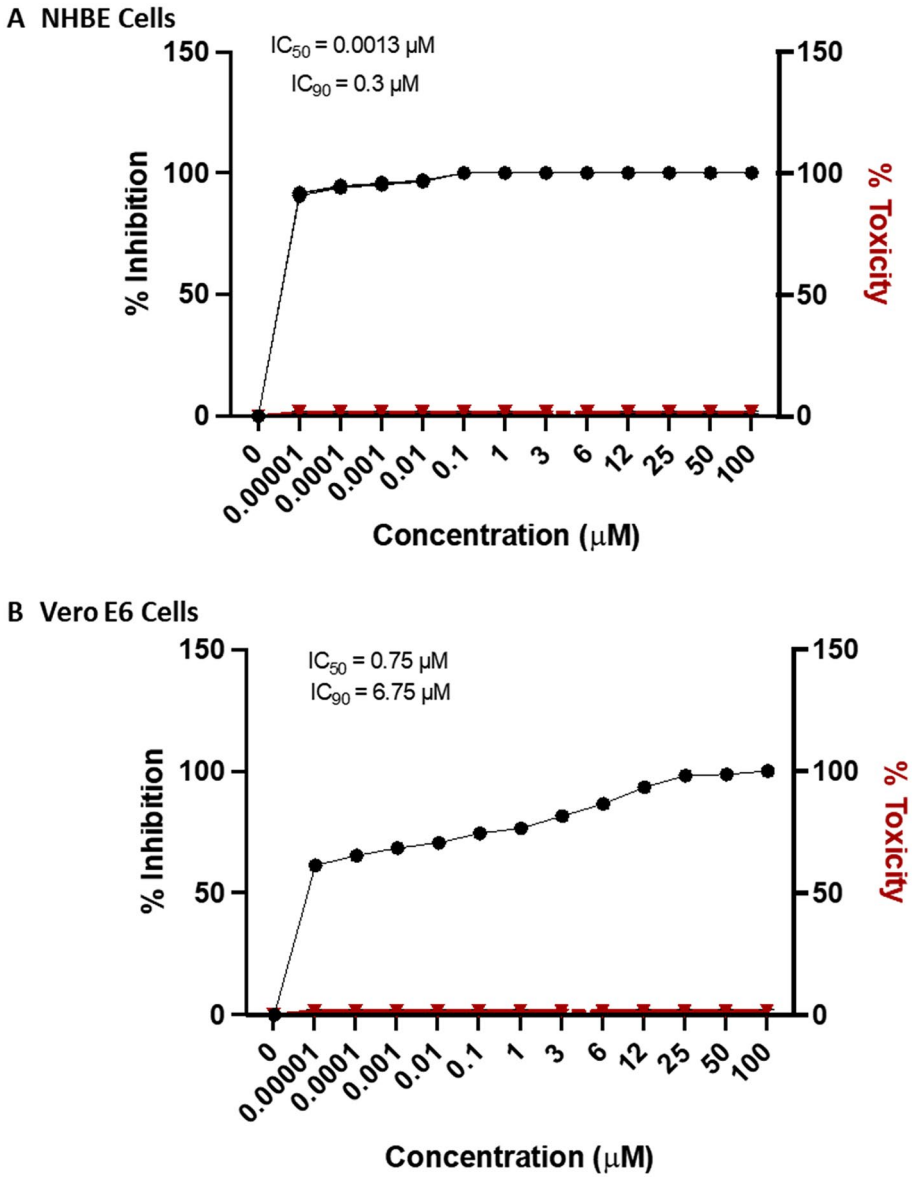

Figure 1. Probenecid potently inhibits SARS-CoV-2 replication in (**A**) NHBE cells and (**B**) Vero E6 cells. IC_{50} and IC_{90} values were calculated in NHBE cells and Vero E6 cells after treating with different probenecid concentrations. Cellular toxicity was calculated in NHBE cells and Vero E6 cells following treatment with different concentrations of probenecid and performing a cell viability assay that measured the percent toxicity based on the conversion of a redox dye (resazurin) into a fluorescent end product (resorufin) after 72 h. Figures were prepared using GraphPad Prism, v9.2, https://www.graphpad.com/updates/.

blockade of OAT3 is safely tolerated in humans[29]. Other compounds that interact with OAT3 include the antiviral drugs oseltamivir phosphate (Tamiflu) and acyclovir[10], as well as angiotensin II receptor blockers[30], however, their interaction is weak and their pharmacological actions confer safety and tolerability limitations that preclude their use in drug repurposing.

Methods

Biosafety. SARS-CoV-2 and variant studies were performed in BSL3 that was approved with relevant ethical regulations for animal testing and research. The hamster study received ethical approval from the University of Georgia IACUC committee and was performed by certified staff in an Association for Assessment and Accreditation of Laboratory Animal Care International-accredited facility. Work followed the institution's guidelines for animal use, the guidelines and basic principles in the NIH Guide for the Care and Use of Laboratory Animals, the Animal Welfare Act, the United States Department of Agriculture, and the United States Public Health Service Policy on Humane Care and Use of Laboratory Animals.

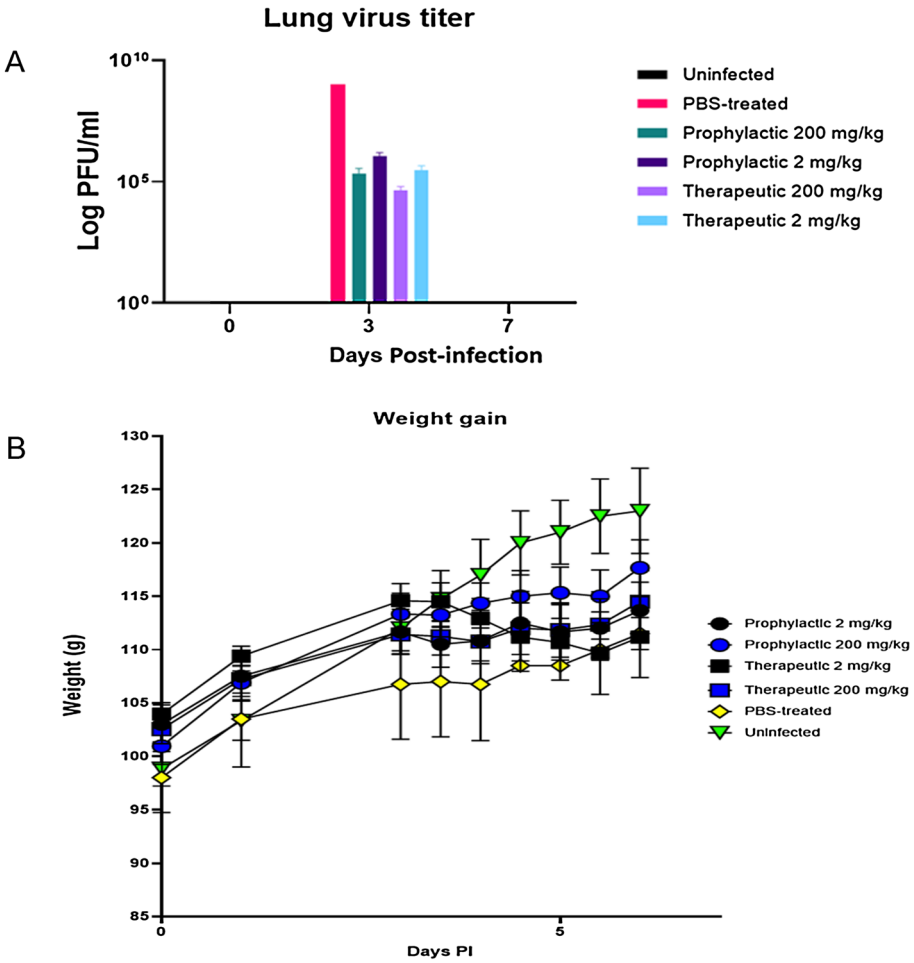

Figure 2. (**A**) Lung virus titers from male hamsters. Hamsters were divided into pre-infection or post-infection groups and i.p. treated with probenecid or PBS (n = 6/group). The groups received 200 mg/kg or 2 mg/kg of probenecid prophylactically at 24 h pre-infection or prophylactically at 48 h pi. The hamsters were i.n. infected with 10^3 PFU of SARS-CoV-2, and at days 3 or 7 pi, the lungs were harvested and virus levels determined by plaque assay. (**B**) Weight gain in hamsters treated prophylactically or therapeutically with 200 mg/kg or 2 mg/kg probenecid. Uninfected hamsters or PBS-treated and infected hamsters were the controls. No substantial weight loss was evident in any of the groups during this study. Figures were prepared using GraphPad Prism, v9.2, https://www.graphpad.com/updates/.

Animals. Male Syrian hamsters were group-housed in HEPA-filtered cage systems enriched with nesting material and were provided with commercial chow and water ad libitum. The animal protocol number for this study was A2020 08-003-Y2-A3, 'Coronavirus infection in the hamster model'. Animals were monitored at least twice daily throughout the study. Hamsters were intranasally infected with 10^3 PFU SARS-CoV-2 (USA-WA1/2020; GenBank: MN985325.1). Hamsters were treated with probenecid (Sigma, St. Louis, MO) 24 h before infection (prophylaxis), or 48 h pi (post-treatment) with doses of 2 mg/kg and 200 mg/kg. All groups were euthanized on day 3 or 7 pi, as day 3–4 pi has been reported as the peak of virus replication[31]. The study is reported in accordance with ARRIVE guidelines.

Hamster study design. Hamsters were divided into pre-infection or post-infection groups and as appropriate were intraperitoneally treated with probenecid (n = 6/group). Groups were treated with 200 mg/kg or 2 mg/kg of probenecid prophylactically at 24 h pre-infection, or prophylactically at 48 h pi. Animal weights were collected once daily and animals were monitored twice daily for disease signs and progression. All procedures were performed on anesthetized animals. Lungs were collected on days 0, 3, and 7 pi for RT-qPCR analysis.

Virus and cells. SARS-CoV-2 isolate nCoV-WA1-2020 (MN985325.1) or the variant (hCoV-19/USA/CA_CDC_5574/2020, B.1.1.7; GenBank: MW422255.1) were received from BEI Resources managed under contract by American Type Culture Collection (ATCC). The viruses were propagated in Vero E6 cells and the cells maintained in high glucose DMEM supplemented with 10% fetal bovine serum and 1 mM L-glutamine.

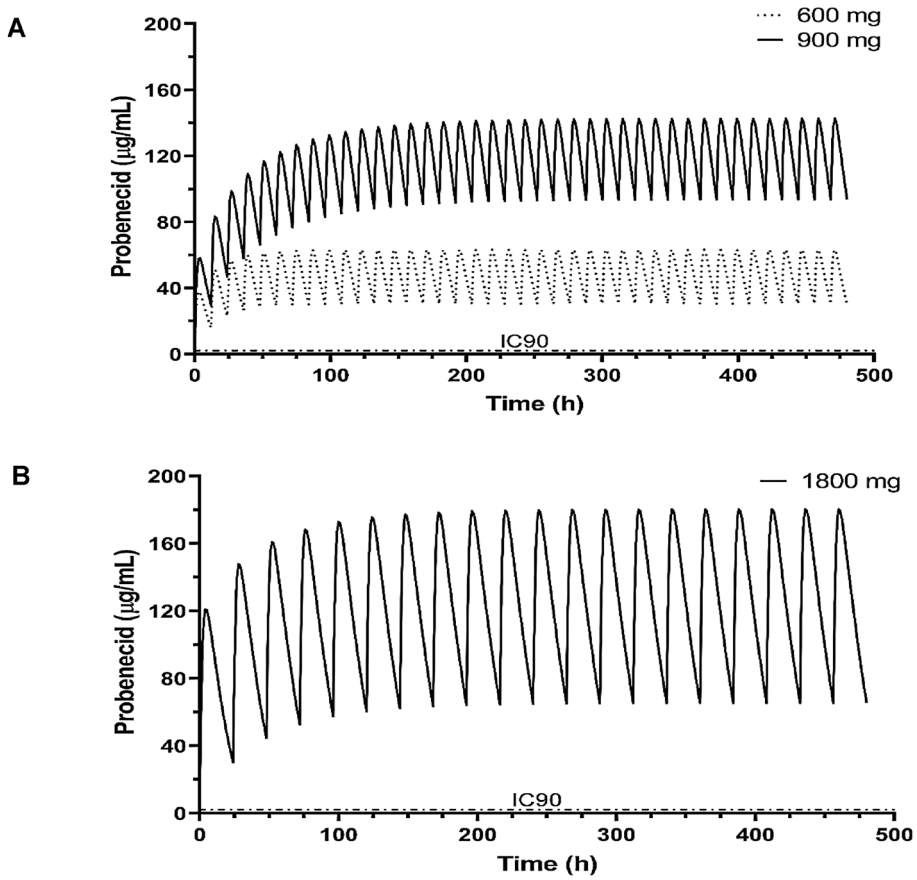

Figure 3. Simulated probenecid concentrations. A population pharmacokinetic model was used to generate probenecid exposure profiles comparing (**A**) 600 mg twice daily, 900 mg twice daily, or (**B**) 1800 mg once daily administration for 20 days. The IC_{90} level corrected for 95% protein binding is 2.08 µg/ml (shown as dashed line). All doses provided exposures well over the IC_{90} level at all time points. Figures were prepared using GraphPad Prism, v9.2, https://www.graphpad.com/updates/.

Dose (mg)	Frequency	Steady state concentration (µg/ml)	Protein binding adjusted IC_{90} value (µg/mL)	Ratio with IC_{90}
600	BID	30.1	2.08	14
900	BID	92.5	2.08	44
1800	QD	64.9	2.08	31

Table 1. Steady state concentration and ratio to protein binding adjusted IC_{90} value after different probenecid doses.

Virus load by RT-qPCR. RNA was extracted from lungs using the QIAamp Viral RNA kit (Qiagen) according to the manufacturer's instructions. Tissues were homogenized and RNA extracted using the RNeasy kit (Qiagen) according to the manufacturer's instructions. RT-qPCR analysis of purified RNA was performed using the CDC EUA N1 probe assay and the CDC EUA human RNaseP internal control probe assay to validate sample RNA extraction in separate reactions.

Virus titration. Virus isolation was performed by inoculating Vero E6 cells in a 96-well plate with a 1:10 dilution series of the virus, and one hour after inoculation of cells, the inoculum was removed and replaced with 0.2 ml TCM. Six days after inoculation, the cytopathogenic effect was scored and the $TCID_{50}$ was calculated using the Reed-Muench method[32].

SARS-CoV-2 in vitro assay. Vero E6 cells (ATCC CRL-1586) were plated in 12-well plates at 5×10^5 cells/well and incubated overnight at 37 °C. Vero E6 cells were washed 1 × with PBS and probenecid (Sigma) was added to the wells in DMEM media and incubated at 37 °C. Each drug concentration was tested in triplicate and the experiment repeated 9 times independently. Following pre-treatment, DMEM media was discarded and cells were replenished with TCM containing probenecid and SARS-CoV-2. Cells were infected at an MOI = 0.01

for 4 days. Post-infection cells were fixed and stained to visualize plaques. Statistical analysis was by one-way ANOVA where $p < 0.05$. NHBE cells were sourced from LONZA (Walkersville, MD) from a non-smoking patient. The cells were seeded at 100,000 cells/T25 flask and incubated at 37 °C. Once cells reached 70–80% confluency, they were dissociated using trypsin and plated using the conditions described above for culture with probenecid.

Modeling and simulation. Probenecid PK data was obtained from a published manuscript[33]. In this study, five adult healthy male subjects (20–39 years, 53–86 kg) were given oral 500, 1000, and 2000 mg probenecid at least one week apart and blood was collected until 48 h. These data were fit in a nonlinear mixed-effects framework using Phoenix NLME software[34]. Parameter estimates for a PK model[33] with saturating (Michaelis–Menten) elimination were used as initial estimates for the current analysis. The model was fitted using the first-order conditional estimation method with an extended least square (FOCE-ELS) algorithm. The base model testing included basic one and two-compartment structures with first-order absorption. Other absorption, lag time, and clearance models were also evaluated. A battery of diagnostic plots was employed to evaluate the adequacy of the goodness of fit for the PK model. The final popPK model was used to simulate exposures resulting from various dosing regimens of potential clinical interest (600 mg BID, 900 mg BID, and 1800 mg QD).

Received: 6 May 2021; Accepted: 19 August 2021
Published online: 10 September 2021

References

1. Oliver, S. E. *et al.* The advisory committee on immunization practices' interim recommendation for use of moderna COVID-19 vaccine—United States, December 2020. *MMWR Morb. Mortal. Wkly. Rep.* **69**, 1653–1656. https://doi.org/10.15585/mmwr.mm695152e1 (2021).
2. Oliver, S. E. *et al.* The advisory committee on immunization practices' interim recommendation for use of Pfizer-BioNTech COVID-19 vaccine—United States, December 2020. *MMWR Morb. Mortal. Wkly. Rep.* **69**, 1922–1924. https://doi.org/10.15585/mmwr.mm6950e2 (2020).
3. Alturki, S. O. *et al.* The 2020 pandemic: Current SARS-CoV-2 vaccine development. *Front. Immunol.* **11**, 1880. https://doi.org/10.3389/fimmu.2020.01880 (2020).
4. Ison, M. G., Wolfe, C. & Boucher, H. W. Emergency use authorization of remdesivir: The need for a transparent distribution process. *JAMA* **323**, 2365–2366. https://doi.org/10.1001/jama.2020.8863 (2020).
5. Hong-Geller, E. & Micheva-Viteva, S. N. Functional gene discovery using RNA interference-based genomic screens to combat pathogen infection. *Curr. Drug Discov. Technol.* **7**, 86–94. https://doi.org/10.2174/157016310793180657 (2010).
6. Tripp, R. A. & Mark Tompkins, S. Antiviral effects of inhibiting host gene expression. *Curr. Top. Microbiol. Immunol.* **386**, 459–477. https://doi.org/10.1007/82_2014_409 (2015).
7. Houzet, L. & Jeang, K. T. Genome-wide screening using RNA interference to study host factors in viral replication and pathogenesis. *Exp. Biol. Med. (Maywood)* **236**, 962–967. https://doi.org/10.1258/ebm.2010.010272 (2011).
8. Orr-Burks, N., Murray, J., Todd, K. V., Bakre, A. & Tripp, R. A. G-protein-coupled receptor and ion channel genes used by influenza virus for replication. *J. Virol.* https://doi.org/10.1128/JVI.02410-20 (2021).
9. Gordon, D. E. *et al.* A SARS-CoV-2 protein interaction map reveals targets for drug repurposing. *Nature* **583**, 459–468. https://doi.org/10.1038/s41586-020-2286-9 (2020).
10. Perwitasari, O. *et al.* Targeting organic anion transporter 3 with probenecid as a novel anti-influenza a virus strategy. *Antimicrob. Agents Chemother.* **57**, 475–483. https://doi.org/10.1128/AAC.01532-12 (2013).
11. Nigam, S. K. *et al.* The organic anion transporter (OAT) family: a systems biology perspective. *Physiol. Rev.* **95**, 83–123. https://doi.org/10.1152/physrev.00025.2013 (2015).
12. Burckhardt, G. Drug transport by organic anion transporters (OATs). *Pharmacol. Ther.* **136**, 106–130. https://doi.org/10.1016/j.pharmthera.2012.07.010 (2012).
13. Burckhardt, B. C. & Burckhardt, G. Transport of organic anions across the basolateral membrane of proximal tubule cells. *Rev. Physiol. Biochem. Pharmacol.* **146**, 95–158. https://doi.org/10.1007/s10254-002-0003-8 (2003).
14. Strilchuk, L., Fogacci, F. & Cicero, A. F. Safety and tolerability of available urate-lowering drugs: a critical review. *Expert. Opin. Drug. Saf.* **18**, 261–271. https://doi.org/10.1080/14740338.2019.1594771 (2019).
15. Woodruff, A. COVID-19 follow up testing. *J. Infect.* **81**, 647–679. https://doi.org/10.1016/j.jinf.2020.05.012 (2020).
16. Washington, N. L. *et al.* Emergence and rapid transmission of SARS-CoV-2 B.1.1.7 in the United States. *Cell* https://doi.org/10.1016/j.cell.2021.03.052 (2021).
17. Driouich, J. S. *et al.* Favipiravir antiviral efficacy against SARS-CoV-2 in a hamster model. *Nat. Commun.* **12**, 1735. https://doi.org/10.1038/s41467-021-21992-w (2021).
18. Bertzbach, L. D. *et al.* SARS-CoV-2 infection of Chinese hamsters (*Cricetulus griseus*) reproduces COVID-19 pneumonia in a well-established small animal model. *Transbound. Emerg. Dis.* https://doi.org/10.1111/tbed.13837 (2020).
19. Boras, B. *et al.* Discovery of a novel inhibitor of coronavirus 3CL protease as a clinical candidate for the potential treatment of COVID-19. *BioRxiv* https://doi.org/10.1101/2020.09.12.293498 (2020).
20. Good, S. S. *et al.* AT-527, a double prodrug of a guanosine nucleotide analog, is a potent inhibitor of SARS-CoV-2 in vitro and a promising oral antiviral for treatment of COVID-19. *Antimicrob. Agents. Chemother.* https://doi.org/10.1128/AAC.02479-20 (2021).
21. Sheahan, T. P. *et al.* An orally bioavailable broad-spectrum antiviral inhibits SARS-CoV-2 in human airway epithelial cell cultures and multiple coronaviruses in mice. *Sci. Transl. Med.* https://doi.org/10.1126/scitranslmed.abb5883 (2020).
22. Rennick, B. R. Renal excretion of drugs: tubular transport and metabolism. *Annu. Rev. Pharmacol.* **12**, 141–156. https://doi.org/10.1146/annurev.pa.12.040172.001041 (1972).
23. Kelley, W. N. & Wyngaarden, J. B. Drug treatment of gout. *Semin. Drug Treat.* **1**, 119–147 (1971).
24. Sahu, G., Sukumaran, S. & Bera, A. K. Pannexins form gap junctions with electrophysiological and pharmacological properties distinct from connexins. *Sci. Rep.* **4**, 4955. https://doi.org/10.1038/srep04955 (2014).
25. Silverman, W., Locovei, S. & Dahl, G. Probenecid, a gout remedy, inhibits pannexin 1 channels. *Am. J. Physiol. Cell Physiol.* **295**, C761-767. https://doi.org/10.1152/ajpcell.00227.2008 (2008).
26. Rosli, S. *et al.* Repurposing drugs targeting the P2X7 receptor to limit hyperinflammation and disease during influenza virus infection. *Br. J. Pharmacol.* **176**, 3834–3844. https://doi.org/10.1111/bph.14787 (2019).

27. Sinha, S. *et al.* In vitro and in vivo identification of clinically approved drugs that modify ACE2 expression. *Mol. Syst. Biol.* **16**, e9628. https://doi.org/10.15252/msb.20209628 (2020).
28. Sharma, K. *et al.* Metabolomics reveals signature of mitochondrial dysfunction in diabetic kidney disease. *J. Am. Soc. Nephrol.* **24**, 1901–1912. https://doi.org/10.1681/ASN.2013020126 (2013).
29. Erdman, A. R. *et al.* The human organic anion transporter 3 (OAT3; SLC22A8): genetic variation and functional genomics. *Am. J. Physiol. Renal. Physiol.* **290**, F905-912. https://doi.org/10.1152/ajprenal.00272.2005 (2006).
30. Sato, M. *et al.* Involvement of uric acid transporters in alteration of serum uric acid level by angiotensin II receptor blockers. *Pharm. Res.* **25**, 639–646. https://doi.org/10.1007/s11095-007-9401-6 (2008).
31. Imai, M. *et al.* Syrian hamsters as a small animal model for SARS-CoV-2 infection and countermeasure development. *Proc. Natl. Acad. Sci. U S A* **117**, 16587–16595. https://doi.org/10.1073/pnas.2009799117 (2020).
32. Pizzi, M. Sampling variation of the fifty percent end-point, determined by the Reed-Muench (Behrens) method. *Hum. Biol.* **22**, 151–190 (1950).
33. Selen, A., Amidon, G. L. & Welling, P. G. Pharmacokinetics of probenecid following oral doses to human volunteers. *J. Pharm. Sci.* **71**, 1238–1242. https://doi.org/10.1002/jps.2600711114 (1982).
34. Javed, H., Meeran, M. F. N., Jha, N. K. & Ojha, S. Carvacrol, a plant metabolite targeting viral protease (M(pro)) and ACE2 in host cells can be a possible candidate for COVID-19. *Front. Plant. Sci.* **11**, 601335. https://doi.org/10.3389/fpls.2020.601335 (2020).

Acknowledgements

The authors would like to thank Phil Young and Billy Meadow for their advice. This work was funded in part by the Georgia Research Alliance and SpinUp Campus.

Author contributions

J.M., R.H., D.M., K.B., and R.T. contributed to the design, data analysis; J.M., D.M., R.T. contributed to the writing of the manuscript; D.M., R.B., and M.L contributed to the probenecid modeling analysis; J.M., R.H. contributed experiment support; D.M. and R.T. contributed to the data analysis; all authors reviewed and contributed to the preparation of the final manuscript.

Competing interests

D.E.M., K.B., F.S., R.S., and R.A.T have ownership in TrippBio. There is no conflict of interest for any authors.

Additional information

Supplementary Information The online version contains supplementary material available at https://doi.org/10.1038/s41598-021-97658-w.

Correspondence and requests for materials should be addressed to R.A.T.

Reprints and permissions information is available at www.nature.com/reprints.

Publisher's note Springer Nature remains neutral with regard to jurisdictional claims in published maps and institutional affiliations.